Reprinted from

surface science

Surface Science 352–354 (1996) 105–111

STM/AFM investigations of β-$MoTe_2$, α-$MoTe_2$ and WTe_2

S.W. Hla [a,c], V. Marinković [b,a,*], A. Prodan [a], I. Muševič [a]

[a] *J. Stefan Institute, P.O. Box 100, 61111 Ljubljana, Slovenia*
[b] *Department of Metallurgy and Materials, University of Ljubljana, Aškerčeva 12, 61000 Ljubljana, Slovenia*
[c] *International Centre for Theoretical Physics, P.O. Box 586, 34100 Trieste, Italy*

Received 5 September 1995; accepted for publication 31 October 1995

ELSEVIER

ELSEVIER

Surface Science 352–354 (1996) 105–111

surface science

STM/AFM investigations of β-$MoTe_2$, α-$MoTe_2$ and WTe_2

S.W. Hla [a,c], V. Marinković [b,a,*], A. Prodan [a], I. Muševič [a]

[a] *J. Stefan Institute, P.O. Box 100, 61111 Ljubljana, Slovenia*
[b] *Department of Metallurgy and Materials, University of Ljubljana, Aškerčeva 12, 61000 Ljubljana, Slovenia*
[c] *International Centre for Theoretical Physics, P.O. Box 586, 34100 Trieste, Italy*

Received 5 September 1995; accepted for publication 31 October 1995

Abstract

There is controversy in the literature concerning the correspondence of STM images to the atomic positions on some transition metal layered dichalcogenide surfaces. Although it is difficult to differentiate between metal and chalcogen atoms in these crystals with hexagonal symmetry, like α-$MoTe_2$, this can be done in cases of β-$MoTe_2$ and WTe_2 with changed metal–Te distances. Contrary to published STM images of WTe_2 our STM images of β-$MoTe_2$ show details which resemble the structure of both corrugated topmost Te and metal layers. The d_{z^2} orbitals of metal atoms protruding vertically upward may provide the tunneling current in this case. The detection of surface or sub-surface atoms depends on the tip electronic condition. The STM results are compared with those from AFM.

Keywords: Atomic force microscopy; Molybdenum ditelluride; Scanning tunneling microscopy; Tungsten ditelluride

1. Introduction

TMD (transition metal dichalcogenide) crystals are widely studied by SPM due to their various potential applications. In general, they are composed of two-dimensional hexagonally packed chalcogen–metal–chalcogen sandwiches with strong covalent bonds inside and weak van der Waals interactions between the sandwiches. Cleavage faces of TMD crystals usually give chalcogen terminated (001) surfaces. Their structures do not differ from terminated bulk structures in many TMD compounds since they are free of dangling bonds and hence do not reconstruct.

In several reports, it is argued that the STM images of TMD surfaces represent metal layers rather than chalcogen ones [1–3]. The dominant part of the wave functions in both valence band top and conduction band bottom of these materials consist of free metal d_{z^2} orbitals which may provide the tunneling current while the chalcogen atomic orbitals are exclusively involved in intralayer bonding. Since both metal and chalcogen layers in most TMD crystals have the same symmetry and in-plane lattice constants (Fig. 1a) and since STM in its topographical mode cannot distinguish between chemical species, it is difficult to decide which atoms are mainly contributing to the STM images.

To clarify this problem, several studies have been carried out on WTe_2 [3–5], in which the structures of Te and W layers are different (Fig. 1b) [6,7]. However, the STM images of WTe_2 surfaces show

* Corresponding author. Fax: +386 61 219 385; e-mail: velibor.marinkovic@ijs.si.

SSDI 0039-6028(95)01106-4

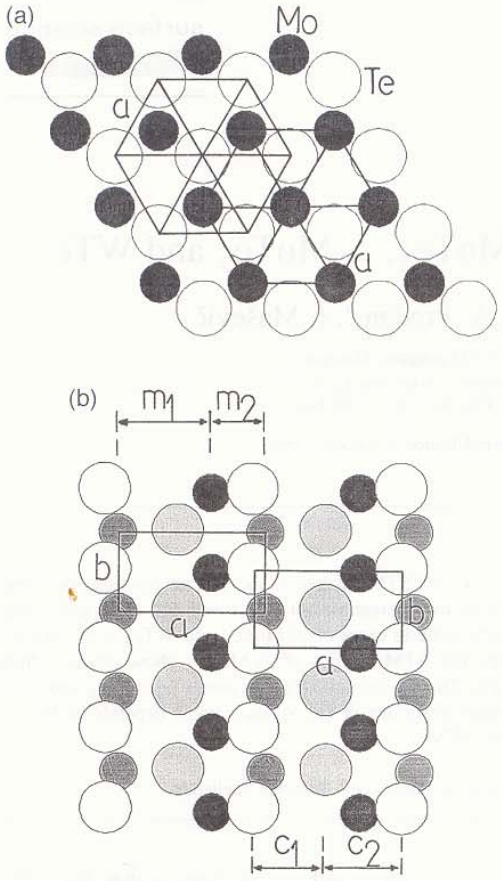

Fig. 1. A schematic drawing of (001) surfaces of (a) α-$MoTe_2$ ($a = 3.519$ Å) (b) β-$MoTe_2$ and WTe_2 where white and gray large circles are top and bottom Te atoms and light and dark small circles are top and bottom metal atoms, respectively. (m_1, m_2 = metal–metal distances in the $x-y$ projected plane with values 4.01 and 2.32 Å for β-$MoTe_2$ and 4.03 and 2.25 Å for WTe_2. c_1, c_2 = Te–Te distances in the $x-y$ projected plane with values 3.11 and 3.22 Å for β-$MoTe_2$ and 3.12 and 3.17 Å for WTe_2.) Unit cell parameters "a" and "b" are 6.33 and 3.469 Å for β-$MoTe_2$ and 6.28 and 3.496 Å for WTe_2.

both Te- and W-layer-like structures which calls for further investigations. The first principles pseudopotential calculation result on WTe_2 shows [4] that the charge distribution of the topmost Te atoms is shifted toward the metal atoms causing a W-layer-like image. Therefore, Te-layer-like and W-layer-like structures in STM images of WTe_2 cannot be definitely ascribed to Te or W atoms. However, according to the same calculation [4], the charge displacement occurs only at the negative sample bias. For the positive sample bias, the charge distributions are almost centered at the actual atomic positions. This is in disagreement with the experiments where the same kind of images [4] are obtained with both sample biases.

To get a better understanding of the STM images of TMD surfaces we investigated α-$MoTe_2$, β-$MoTe_2$ and WTe_2(001) surfaces by AFM and STM. α- and β-$MoTe_2$ have been chosen because of their chemically identical but structurally different nature [6,7]. In addition, experiments on WTe_2 were included to be compared with published results and due to the structural similarities of the (001) surfaces of WTe_2 and β-$MoTe_2$.

2. Experimental

All crystals were grown by chemical vapor transport in evacuated silica tubes with I_2 as the transport agent. Their structures were confirmed by XRD measurements. The samples were cleaved with an adhesive tape just before the experiments. STM investigations were performed using an Omicron UHV STM system with an operating pressure between 10^{-10} and 10^{-11} mbar. The STM was operated in the constant current mode. Electrochemically etched tungsten tips were used throughout this work. The quality of each tip was pre-examined by scanning a test image on graphite prior to each experiment.

AFM examinations were performed with a Digital Instruments Nanoscope III SPM system in air in the contact and lateral force modes and silicon nitride cantilevers were used. Mica was used for adjustment of the AFM scanner and to check the quality of the cantilever.

3. Results and discussion

3.1. α-$MoTe_2$

Atomic resolution STM images of α-$MoTe_2$ were obtained with both positive and negative polarities of

the sample varying from +0.5 to +2.5 V and from −0.3 to −3 V, respectively. The tunneling currents were within the range from 0.5 to 4 nA. There was virtually no atomic resolution obtained from −0.3 to 0.5 V which approximately corresponds to the band gap of this material [6]. Fig. 2a and Fig. 2b show STM and AFM images of α-$MoTe_2$ surface. Contrary to the AFM image of the α-$MoTe_2$, the STM image contains both metal and chalcogen charge density contributions. Several published STM images of TMD surfaces, such as MoS_2 and $NbSe_2$ [8], also show both chalcogen and metal contributions. Though, one cannot distinguish between chalcogen and metal charge densities in these images, they certainly prove that the metal d_{z^2} orbitals can penetrate outward and can provide tunneling current.

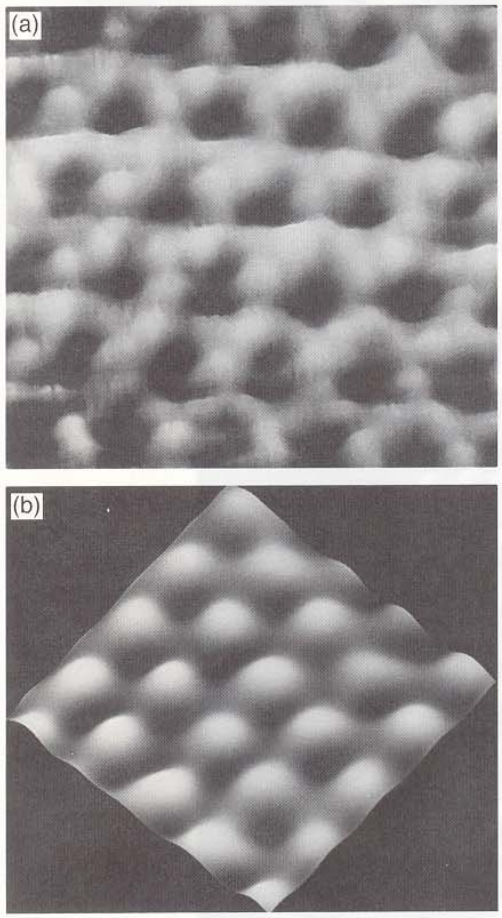

Fig. 2. (a) A 16×16 Å^2 STM image (I_t = 3.5 nA, U_t = 5 mV) of α-$MoTe_2$ where both Mo and Te contributions are visible and (b) corresponding AFM image (15×15 Å^2) taken in contact mode.

3.2. β-$MoTe_2$

The STM images of (001) β-$MoTe_2$ surfaces were taken with tip-to-sample bias voltage ranging from −0.3 mV to −1 V and +0.3 mV to +1 V. The tunneling current range was between 0.03 and 45 nA.

The reduction of Mo–Mo bond lengths in β-$MoTe_2$ as compared with that of α-$MoTe_2$ causes indirect band overlapping which results in a semimetallic behavior [6]. This is reflected in STM imaging, where good atomic resolution can be obtained even with very low bias voltage (±0.3 mV) which is not the case for semiconducting α-$MoTe_2$. The best atomic resolutions are obtained with bias voltages from +0.3 mV to +0.5 V and −0.3 mV to −1 V.

The STM images of β-$MoTe_2$ resemble either the atomic configuration of the topmost Te layer (Fig. 3a) or the subsurface Mo layer (Fig. 3b) or combinations of both. All three kinds of images were observed for both positive and negative sample voltages while the AFM image (Fig. 3c) shows the expected chalcogen surface topography. Different images appear more often at reduced bias voltages (close to the Fermi level) especially within +0.3 mV to 3 V and −0.3 mV to −3 V regions. Since the density of states (DOS) for β-$MoTe_2$ contains both metal "d" and chalcogen "p" energy levels close to the Fermi level [6], it is possible that both atoms contribute to the tunneling current at suitable circumstances.

To determine the influence of the tip-to-sample distance in this case, STM images were recorded by varying the tunneling current between 0.03 and 45 nA at each bias voltage. It was found that with the tip far away from the surface (I_t below 0.5 nA), only Te-layer-like images were observed at both bias voltage polarities. With the tip closer to the surface (I_t between 0.5 and 3.5 nA), both Mo-layer-like and Te-layer-like images were observed with approximately equal frequency.

This can be explained as follows: with the tip far away from the surface, the subsurface metal d_{z^2} orbitals are at a larger distance from the tip than the surface chalcogen "p" orbitals and hence they do not overlap with the tip wavefunctions. Since only the wavefunctions from the chalcogen "p" orbitals overlap with the tip wavefunctions at this stage, all the images are Te-layer-like. When the tip is close enough to the surface, the free metal d_{z^2} orbitals can also contribute to the tunneling current.

In Fig. 4, showing the STM image of β-$MoTe_2$ taken at $U_g = 0.7$ mV and $I_t = 1.2$ nA, both Te and metal layers are visible. In this image, average measured distances between the bright spots are close to the metal–metal distances while the distances between the fainter ones are close to the chalcogen–

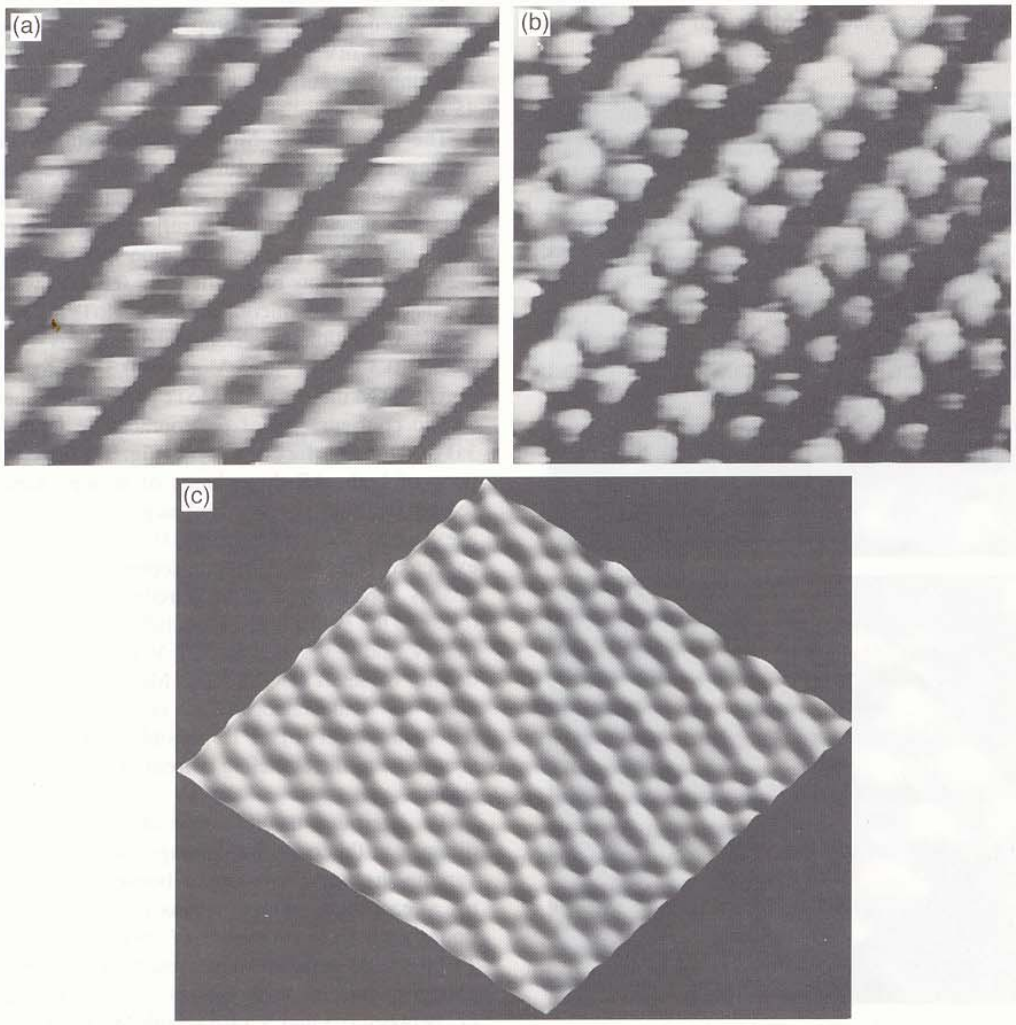

Fig. 3. β-$MoTe_2$ (001) surface. (a) 22×22 Å^2 Te-layer-like image ($U_t = -1$ mV, $I_t = 0.5$ nA), (b) 18×18 Å^2 Mo-layer-like image ($U_t = +1$ mV, $I_t = 3$ nA), (c) corresponding AFM image (75×75 Å^2) acquired in contact mode.

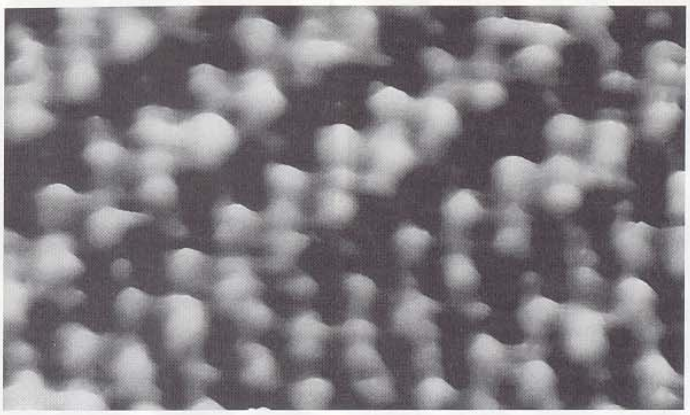

Fig. 4. A STM image (37×22 Å^2) of β-$MoTe_2$ showing both Mo and Te contributions.

chalcogen distances ($m_1 = 3.96$ Å, $m_2 = 2.24$ Å, $c_1 = 3.06$ Å and $c_2 = 3.18$ Å as compared with Fig. 1). This image proves that the contribution of the metal charge density to the tunneling current can be higher than that of the chalcogens under certain conditions. Fig. 5 demonstrates the change from Te-layer-like image to metal-layer-like image after a scan artefact.

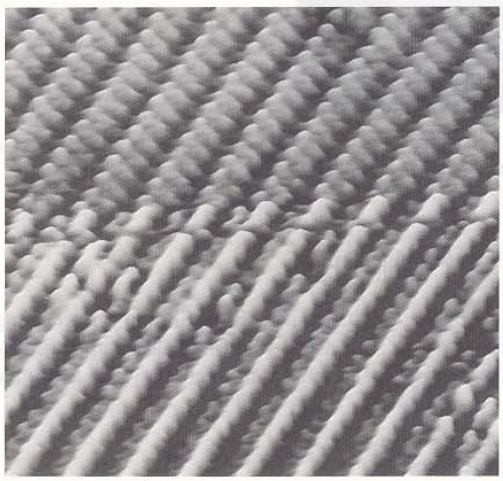

Fig. 5. A 80×80 Å^2 STM image of β-$MoTe_2$ ($U_t = +0.3$ mV, $I_t = 1.5$ nA). Note the change from a Te-layer-like into a Mo-layer-like image.

3.3. WTe_2

The STM images of WTe_2 were obtained at almost the same tunneling parameters as those of β-$MoTe_2$. Fig. 6a and Fig. 6b show the Te- and W-layer-like images of the WTe_2 (001) surface and Fig. 6c is the corresponding AFM image. As in case of β-$MoTe_2$, only Te-layer-like images are observed with the tip far from the surface and both types of images can be observed for close enough tips. These observations are independent of specimen bias voltage polarities in contrast with the calculated result [4], according to which W-layer-like images can be observed only at negative sample biases.

4. Conclusions

1. The AFM images of α-$MoTe_2$, β-$MoTe_2$ and WTe_2 show expected chalcogen surface topographies while the corresponding STM images contain chalcogen or metal or both chalcogen and metal contributions. This is due to the free metal d_{z^2} orbitals which provide tunneling current at certain conditions.
2. In cases of β-$MoTe_2$ and WTe_2, the observation of the metal- and chalcogen-like structures does not depend on the sample biases since both can be observed at positive as well as negative biases.

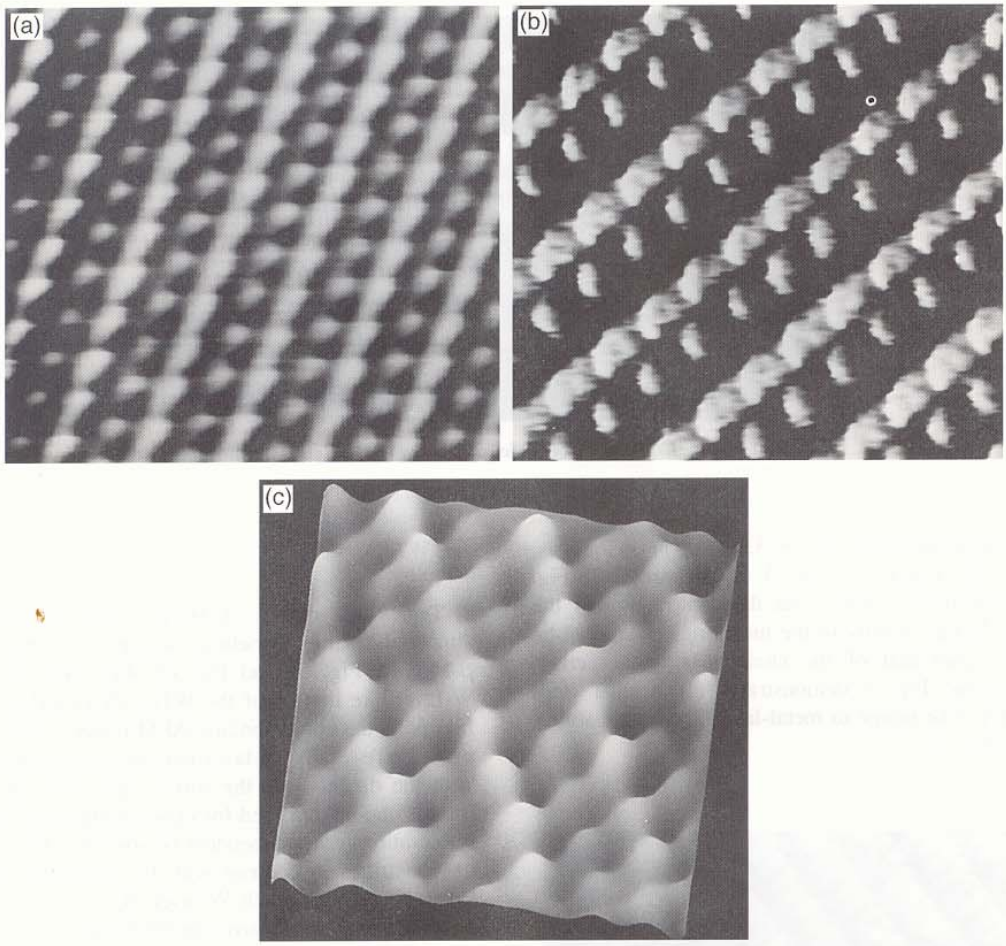

Fig. 6. (001) WTe_2 surface. (a) 37×32 Å^2 Te-layer-like image ($U_t = +1.5$ mV, $I_t = 3.5$ nA), (b) 30×25 Å^2 W-layer-like image ($U_t = +0.8$ mV, $I_t = 3$ nA) and (c) corresponding AFM image taken in the lateral force mode (21×21 Å^2).

3. Present experiments show that chalcogen as well as metal atoms can contribute to the STM images of TMD surfaces depending on the tip-to-sample distance.
4. In addition, the two types of images can switch from one into the other during a single scan. Imaging of metal or chalcogen atoms depends on the tip conditions. The tip structure and corresponding electronic states may change during scanning and create conditions for imaging either metal or chalcogen atoms.

Acknowledgements

Thanks are due to Mrs. Zora Škraba for preparing the crystals. This work was financially supported by the Ministry of Science and Technology of Slovenia.

References

[1] G.W. Stupian and M.S. Leung, Appl. Phys. Lett. 51 (1987) 1560.

[2] S. Akari, M. Stachel, H. Birk, E. Schreck, M. Lux and K. Dransfeld, J. Microsc. 152 (1988) 521.
[3] S.L. Tang, R.V. Kasowski and B.A. Parkinson, Phys. Rev. B 39 (1989) 9987.
[4] S.L. Tang, R.V. Kasowski, A. Suna and B.A. Parkinson, Surf. Sci. 238 (1990) 280.
[5] A. Crossley, S. Myhra and C.J. Sofield, Surf. Sci. 318 (1994) 39.
[6] W.G. Dawson and D.W. Bullett, J. Phys. C 20 (1987) 6159.
[7] B.E. Brown, Acta Cryst. 20 (1966) 268.
[8] K. Uozumi, K. Nakamoto and K. Fujioka, Jpn. J. Appl. Phys. 27 (1988) L123;M. Weimer, J. Kramer, C. Bai and J.D. Baldeschwieler, Phys. Rev. B 37 (1988) 4292.